A nonequilibrium force can stabilize 2D active nematics

Ananyo Maitra[a,1], Pragya Srivastava[b], M. Cristina Marchetti[c], Juho S. Lintuvuori[d], Sriram Ramaswamy[e,f], and Martin Lenz[a,g,1]

[a]LPTMS, CNRS, Université Paris-Sud, Université Paris-Saclay, 91405 Orsay, France; [b]Theoretical Physics of Biology Laboratory, The Francis Crick Institute, London NW1 1AT, United Kingdom; [c]Physics Department, Soft and Living Matter Program, Syracuse University, Syracuse, NY 13244; [d]Université Bordeaux, CNRS, LOMA, UMR 5798, F-33405 Talence, France; [e]Tata Institute of Fundamental Research Centre for Interdisciplinary Sciences, Hyderabad 500107, India; [f]Centre for Condensed Matter Theory, Department of Physics, Indian Institute of Science, Bangalore 560012, India; and [g]MultiScale Material Science for Energy and Environment, Unité Mixte Internationale 3466, CNRS-Massachusetts Institute of Technology, Cambridge, MA 02139

Suspensions of actively driven anisotropic objects exhibit distinctively nonequilibrium behaviors, and current theories predict that they are incapable of sustaining orientational order at high activity. By contrast, here we show that nematic suspensions on a substrate can display order at arbitrarily high activity due to a previously unreported, potentially stabilizing active force. This force moreover emerges inevitably in theories of active orientable fluids under geometric confinement. The resulting nonequilibrium ordered phase displays robust giant number fluctuations that cannot be suppressed even by an incompressible solvent. Our results apply to virtually all experimental assays used to investigate the active nematic ordering of self-propelled colloids, bacterial suspensions, and the cytoskeleton and have testable implications in interpreting their nonequilibrium behaviors.

active matter | living liquid crystals | confined active nematics

Living systems convert chemical energy into motion, thus violating detailed balance at the microscopic scale. Macroscopically, these violations result in stresses and currents responsible for intracellular flows leading to cellular motion (1), collective cell migration during embryonic development (2), and the flocking of birds (3). Similar nonequilibrium currents arise in nonliving systems such as chemotactic colloids (4) and vibrated granular rods (5). These systems are often described by active hydrodynamic theories, a class of continuum descriptions derived from equilibrium theories of liquid crystals but supplemented with extra "active" forces arising from microscopic driving (6–8). These theories are tools of choice to study specifically nonequilibrium features in the collective behaviors of fluid suspensions of anisotropic active units such as cytoskeletal filaments (9, 10) or bacteria (11).

A central issue in active hydrodynamics is to determine the effects of activity on the dynamic stability and the robustness against fluctuations of various types of orientational and translational order. Previous studies have shown that, due to the interplay of active stress and solvent flow, nematic order in incompressible active suspensions is always unstable beyond a critical value of activity (7, 8, 12–14). This instability threshold vanishes in the limit of infinite system size, implying that, unlike their equilibrium counterparts, these systems are generically unstable. In 2D experimental realizations this instability can, however, be suppressed by the friction of the fluid against a substrate. Nevertheless, current theories predict that even under these conditions instability always occurs at high enough activity (15), which may be experimentally realized through an increase of the density of myosin motors or bacteria or of the amount of fuel available to them.

Another distinctive feature of active systems is the statistics of their density fluctuations. In equilibrium systems away from critical points and with finite-range interactions, a region of space containing N particles on average will undergo fluctuations of this number of order $\sqrt{N}$ whether or not it is embedded in an incompressible solvent. In contrast, active hydrodynamic theories of systems without incompressibility display fluctuations of order greater than $\sqrt{N}$ due to active mass currents arising from orientation fluctuations (5, 7, 8, 16, 17). While these so-called giant number fluctuations have clearly been observed in solventless settings, little is known about their form in the presence of an incompressible solvent (18), and their observation in biological experiment has been difficult and controversial (19).

To help interpret the rich dynamical behavior of typically quasi-2D experiments on active systems (10, 11, 19, 20) here we study theoretically the ordering and fluctuations of an apolar active fluid in contact with a substrate. By reexamining the foundation of active hydrodynamic theories in two dimensions, we first find that the contact with a substrate allows an extra active force with a distinct angular symmetry. This force does not conserve angular momentum, yet it exists even in achiral systems. Contrary to common wisdom, increased activity in the presence of this term can lead to a stabilization of nematic ordering. Here, we first qualitatively discuss the geometrical meaning of this extra force and derive its form from symmetry considerations in a purely 2D system. We next show that giant number fluctuations in the active nematic phase are robust to the introduction of incompressible solvent as well as this active force. Finally, we show that this potentially stabilizing active force emerges

Significance

Living systems differ from dead matter in one crucial aspect: They are driven by internal engines. In anisotropic fluids, the widely accepted framework of active matter theory predicts that this necessarily leads to an instability from quiescence to large-scale and eventually incoherent motion. Here we challenge this common wisdom by reexamining the symmetries of the most ubiquitous experimental geometry for active systems. We uncover an additional coupling between activity and motion that can make an active system even more stable than its passive counterpart, while preserving other hallmarks of nonequilibrium physics. Our results challenge common views on active matter and clarify the interpretation of multiple experiments.

[1]To whom correspondence may be addressed. Email: ananyo.maitra@u-psud.fr or martin.lenz@u-psud.fr.

This article contains supporting information online at www.pnas.org/lookup/suppl/doi:10.1073/pnas.1720607115/-/DCSupplemental.

naturally from an accepted model of 3D active fluid under vertical confinement and argue that it is the dominant active force in a renormalized theory in the presence of noise. Our results offer plausible explanations for the persistence of order at high activity, as well as the systematics of instabilities, in bacterial, living liquid crystal, and cytoskeletal systems.

Qualitative Argument

The well-known destabilization of an active nematic is a result of particles exerting dipolar force distributions of either sign on the solvent surrounding them. As illustrated in Fig. 1 *A* and *B*, dipolar force distributions of either sign always destabilize the ordered state. The core of our argument consists of remarking that unlike these dipolar distributions, force distributions of higher angular symmetry do not generically destabilize the ordered phase. To see this, consider the square shape with quadrupolar force distribution shown in Fig. 1*C*, which pulls fluid perpendicular to its faces and pushes it out of its corners. Perturbing a perfectly aligned row of particles exerting this more symmetric active force density leads to a bunching of their corners in some locations, which reinforces their pushing of the fluid, and a spreading out in others. As a result, fluid tends to flow from the spread-out to the bunched-up regions, i.e., in the direction opposite to that pictured in Fig. 1*A*, which pushes the particles back toward the perfectly aligned state. Moreover, the fourfold symmetry of the particles prevents them from distinguishing between splay and bend perturbations. As a result, their activity—if of the right sign—always helps stabilize the aligned state.

Beyond these schematic examples, the force distribution in an active nematic generically has both dipolar and higher symmetry contributions. However, in active systems such as suspended films and 3D bulk fluids where momentum is conserved, all higher symmetry contributions are subdominant to the dipolar one at large scales. Here, we show that this is not the case in 2D systems on a substrate as well as 3D fluids under vertical confinement. As a result, depending on its magnitude and sign the higher angular symmetry active force can lead to an overall stabilization of the active fluid, in contradiction with the widely held view that incompressible active nematics are always unstable at high activity.
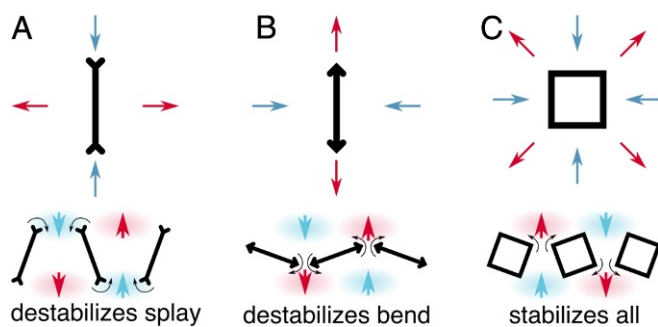

Fig. 1. Active forces influence the stability of an orientable fluid. (*A*, *Top*) A nematic "puller" aspirates the surrounding solvent along its long direction (blue arrows) to reject it along the short direction (red arrows). (*A*, *Bottom*) The splayed configuration thus results in the solvent flows shown by the thick arrows, which drag the particles along and thus accentuate the original disturbance by rotating them as indicated by the thin arrows. (*B*) "Pushers" with the opposite force dipole, while stable against splay, are unstable when in a bend configuration. (*C*) The active force introduced here is also present in nematic active systems, but is associated with higher multipoles of the force density distributions. In the example shown here, the resulting flow consistently stabilizes the ordered state of the particles. We show that for systems on a substrate this active stabilization can overcome the well-characterized destabilization associated with the dipolar terms.

Model for Active Nematic Suspension on a Substrate

We now offer a formal description of the dynamics of the local orientation $\theta(\mathbf{r}, t)$ and velocity $\mathbf{v}(\mathbf{r}, t)$ of our nematically ordered 2D active suspension, as well as the concentration $c(\mathbf{r}, t)$ of its active particles.

Dynamics of the Orientation Field. Considering small deviations from a homogeneous state aligned along $\hat{\mathbf{x}}$, we write the linear dynamical equations compatible with the symmetries of the system in the long-wavelength (hydrodynamic) limit. The dynamical equation for the angle field is

$$\dot{\theta} = \frac{1-\lambda}{2}\partial_x v_y - \frac{1+\lambda}{2}\partial_y v_x - \Gamma_\theta \frac{\delta \mathcal{H}}{\delta \theta}, \qquad [1]$$

where $|\lambda| > 1$ describes particles with a tendency to align under a shear flow (e.g., cytoskeletal filaments) while $|\lambda| < 1$ denotes flow tumbling (as in bacteria). Here we use the simplified one-Frank-constant free-energy functional

$$\mathcal{H} = \int d^2\mathbf{r} \left[\frac{K}{2}(\nabla \theta)^2 + g(c) \right], \qquad [2]$$

where $K > 0$ characterizes the tendency of the particles to align and $g(c)$ is an arbitrary function of the concentration.

Flow Field and Active Forces. Flow is driven by forces internal to the fluid, and the presence of the substrate dictates Darcy dynamics,

$$\Gamma \mathbf{v} = -\nabla \Pi + \mathbf{f}^p + \mathbf{f}^a, \qquad [3]$$

where Γ can be viewed as the friction coefficient against the substrate. The pressure Π serves as a Lagrange multiplier enforcing the incompressibility condition $\nabla \cdot \mathbf{v} = 0$ for the suspension as a whole, while still permitting fluctuations in the concentration of suspended particles. We do not consider the case of a compressible medium, which adds no physics of interest. Onsager symmetry and Eq. **1** yield the density of passive (equilibrium) forces

$$\mathbf{f}^p = -\frac{1+\lambda}{2}\partial_y \left(\frac{\delta \mathcal{H}}{\delta \theta} \right)\hat{\mathbf{x}} + \frac{1-\lambda}{2}\partial_x \left(\frac{\delta \mathcal{H}}{\delta \theta} \right)\hat{\mathbf{y}}. \qquad [4]$$

Beyond these standard equilibrium terms, the active force density $\mathbf{f}^a$ depends on θ only through its gradient due to rotational invariance. Combining this with the $(x, y, \theta) \to (x, -y, -\theta)$ reflection invariance of our achiral system dictates that to lowest order in gradients

$$f_x^a = -(\zeta_1 \Delta\mu + \zeta_2 \Delta\mu)\partial_y \theta \qquad [5a]$$
$$f_y^a = -(\zeta_1 \Delta\mu - \zeta_2 \Delta\mu)\partial_x \theta, \qquad [5b]$$

where ζ_1 and ζ_2 are two independent, a priori unknown phenomenological constants, and $\Delta\mu$ denotes the strength of the overall activity in the system, e.g., the chemical potential difference between the cellular fuel ATP and its hydrolysis products. We interpret the two components of $\mathbf{f}^a$ in Fig. 2, with f_x^a inducing a horizontal fluid flow in a splayed nematic while f_y^a drives a vertical fluid flow in a bent nematic. An active force depending on gradients of c is also allowed in $\mathbf{f}^a$, but does not significantly modify our discussion (*SI Appendix, IA. Dynamics on a Substrate*). While the active force proportional to ζ_1 is standard in active fluid theories, the present work introduces and explores the effect of the solenoidal ζ_2 force.

This force can be understood in simple terms by introducing the nematic director $\mathbf{n} = (\cos\theta, \sin\theta)$. In momentum-conserving systems, the active force can be only the divergence of a symmetric stress, namely $\mathbf{f}^a = \zeta_1 \Delta\mu \nabla \cdot (\mathbf{nn}) = \zeta_1 \Delta\mu[\mathbf{n}(\nabla \cdot \mathbf{n}) + \mathbf{n} \cdot \nabla\mathbf{n}]$.

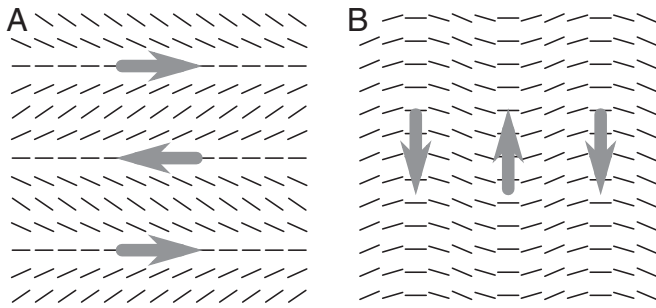**Fig. 2.** The two components of the active force $\mathbf{f}^a$ determine the stability of the active nematic with respect to splay and bend. (*A*) A splay perturbation $\partial_y\theta \neq 0$ (black segments) induces an active force $f_x^a = a\partial_y\theta$ which stabilizes a flow-tumbling system if $a < 0$ (represented by the arrows). (*B*) A bend perturbation $\partial_x\theta \neq 0$ produces an active force $f_y^a = b\partial_x\theta$ which stabilizes a flow-tumbling system if $b > 0$.

The ζ_2 force involves an exchange of angular momentum with the substrate, and introducing it thus allows an active force with different prefactors for the terms $\mathbf{n}(\nabla \cdot \mathbf{n})$ and $\mathbf{n} \cdot \nabla\mathbf{n}$. The form of active force density we propose also has the same symmetry as the general flexoelectric polarization in nematic liquid crystals, whereas $\nabla \cdot (\mathbf{nn})$ is analogous to a more restricted case in which the magnitudes of the polarization for a bend and a splay deformation of equal strength are the same (21, 22). Since a local polarization in a system out of equilibrium may be associated with a local force density, this analogy provides a further heuristic justification for Eq. **5**.

Concentration Dynamics. The evolution of the concentration c is governed by a conservation equation $\partial_t c = -\nabla \cdot (\mathbf{J}^p + \mathbf{J}^a)$, where the passive particle current reads $\mathbf{J}^p = -\Gamma_c\nabla\delta\mathcal{H}/\delta c$. As with $\mathbf{f}^a$, the active current $\mathbf{J}^a$ comprises two distinct θ-dependent active terms a priori, but the term analogous to ζ_2, being a curl, drops out of the conservation equation, yielding

$$\partial_t c = \Gamma_c\nabla^2\frac{\delta\mathcal{H}}{\delta c} + \zeta_c\Delta\mu\partial_x\partial_y\theta, \qquad [6]$$

where the $\zeta_c\Delta\mu$ active term couples orientation fluctuations with concentration fluctuations and is featured in standard theories of active nematics (7, 16).

Active Stabilization of the Ordered Phase

The active term $\zeta_2\Delta\mu$ has dramatic consequences for the linear stability of the active fluid. Consider the evolution of a small perturbation $\theta_\mathbf{q}e^{i\mathbf{q}\cdot\mathbf{x}}$ with a wave vector $\mathbf{q} = q(\cos\phi\,\hat{\mathbf{x}} + \sin\phi\,\hat{\mathbf{y}})$. Combining Eqs. **1**–**6** and eliminating pressure by projecting on the direction perpendicular to $\mathbf{q}$, we find that the dynamics are diffusive to leading order in q: $\partial_t\theta_\mathbf{q} = -D(\phi)q^2\theta_\mathbf{q}$, where the direction-dependent orientational diffusivity is given by

$$D(\phi) = \Gamma_\theta K + \frac{\Delta\mu}{2\Gamma}(1 - \lambda\cos 2\phi)(-\zeta_1\cos 2\phi + \zeta_2). \qquad [7]$$

The system is thus linearly stable at small q if and only if $D(\phi)$ is positive for all values of ϕ, i.e., if the second term in the right-hand side of Eq. **7** is not so large as to overcome the stabilizing effect of director relaxation through $\Gamma_\theta K$. We now focus on this second term, which dominates for high activity, i.e., large $\Delta\mu$. The case of flow-tumbling ($|\lambda| < 1$) systems, where $(1 - \lambda\cos 2\phi)$ is always positive, is easy to interpret as it is controlled by the active force $\mathbf{f}^a$. As shown in Fig. 2, splay can be stabilized by a force f_x^a that depends on $\partial_y\theta$ only through a negative coefficient, whereas bend stabilization requires f_y^a to depend on

$\partial_x\theta$ through a positive coefficient. As previous studies implicitly assume $\zeta_2 = 0$, Eq. **5** clearly shows that they impose the equality of these two coefficients, implying a destabilization of either bend or splay, depending on its sign. The introduction of the active force ($\zeta_2 \neq 0$) now offers the possibility for these coefficients to have opposite signs. For $\zeta_2 > |\zeta_1|$ this implies that the stability of the system, i.e., a positive relaxation rate, increases with increasing activity, as shown in Fig. 3*A*. By contrast, Fig. 3 shows that both flow-aligning ($|\lambda| > 1$) and $\zeta_2 < |\zeta_1|$ systems remain generically unstable at high activity.

Giant Number Fluctuations

Having opened up the possibility of a stable homogeneous nematic at high activity, we now examine the nature of concentration fluctuations arising in such a state when nonconserving and conserving noise sources are added to Eqs. **1** and **6**, respectively. We find that the giant number fluctuations persist despite the long-range effects associated with the incompressible velocity field. This result, which is in clear contrast to the case of incompressible active polar systems (23), can be seen without a detailed calculation by examining the structure of Eqs. **6** and **7**. Indeed, compared with compressible nematic systems, incompressibility introduces only a nonsingular anisotropy in the orientational relaxation rate Eq. **7**, without modifying the scaling with wavenumber. Since giant number fluctuations rely solely on the wavenumber scaling of the orientational relaxation rate and not on its anisotropy (16), they should be present in our system as well. Specifically, simple power counting within a linearized treatment demonstrates that, due to the active concentration current, concentration fluctuations $\delta c = c - \langle c \rangle$ scale with q in the same way as orientation fluctuations. Therefore, the static structure factor $\mathcal{S}_\mathbf{q} \equiv \int_\mathbf{r}\langle\delta c(\mathbf{0})\delta c(\mathbf{r})\rangle\exp(-i\mathbf{q}\cdot\mathbf{r})/\langle c\rangle$ of concentration fluctuations scales as $1/q^2$. Equivalently, in a region containing on average N particles, the SD in the number scales linearly with N in two dimensions. Only the form of the predicted anisotropy of $\mathcal{S}_\mathbf{q}$ is modified (*SI Appendix, IA. Dynamics on a Substrate*) with respect to that in ref. 16, due to the factor $D(\phi)$ in Eq. **7**. Our conclusions remain valid even upon inclusion of more general symmetry-allowed active and passive terms (*SI Appendix, IA. Dynamics on a Substrate*).

Emergence of the Additional Active Force in Confined Active Nematics

To further elucidate the physical origin of our active force, we consider the dynamics of a 3D active suspension of lateral
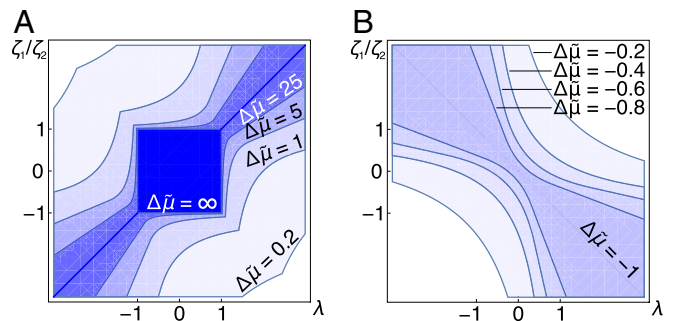

Fig. 3. Regions of stability of the ordered phase as given by the sign of $D(\phi)$ in Eq. **7** as a function of the flow-alignment parameter λ, the ratio ζ_1/ζ_2 of the two active forces, and the overall magnitude of activity relative to passive friction $\Delta\tilde{\mu} = \zeta_2\Delta\mu/2K\Gamma\Gamma_\theta$. (*A*) For $\Delta\tilde{\mu} > 0$, the region of linear stability of the ordered phase (shades of blue) shrinks with increasing activity, yet the central dark blue square is stable for arbitrary high activity. (*B*) For $\Delta\tilde{\mu} < 0$, stability is abolished for large enough activity, namely $\Delta\tilde{\mu} < -1$.

dimension L confined over a length scale $h \ll L$ in the z direction and project it onto a 2D xy plane. To perform this operation, we use a standard lubrication approximation correct in the limit of small h/L (24, 25). This approximation is based on a separation of scale between the gradients and velocities within and perpendicular to the xy plane, namely $\bar{\partial}_z \gg (\bar{\partial}_x, \bar{\partial}_y)$ and $\bar{v}_z \ll (\bar{v}_x, \bar{v}_y)$, where the bar denotes 3D variables and operators. The 2D flow equations are then obtained by averaging each term in the 3D flow equations over the thickness of the confined fluid. We illustrate this procedure by averaging the 3D viscous force density $\bar{\nabla}^2 \bar{\mathbf{v}}$ found in both the standard Navier–Stokes equation and the flow equation for a full 3D active fluid. We consider a simple Poiseuille profile $\bar{\mathbf{v}}_\perp(x, y, z) = (4/h^2) z(h - z)\bar{\mathbf{v}}_0(x, y)$ for the vertical structure of the flow, where $\bar{\mathbf{v}}_\perp = (\bar{v}_x, \bar{v}_y)$ is the projection of the 3D velocity vector in the xy plane, $\bar{\mathbf{v}}_0(x, y)$ is its value in the midplane, and where a no-slip condition is imposed on the bounding surfaces at $z = 0$ and $z = h$. Denoting by $\mathbf{v}(x, y) = (2/3)\bar{\mathbf{v}}_0(x, y)$ the z-averaged velocity we find that the thickness-averaged viscous force density reads

$$\frac{1}{h}\int_0^h \bar{\eta}\bar{\nabla}^2 \bar{\mathbf{v}}_\perp \, dz = -\frac{12\bar{\eta}}{h^2}\mathbf{v} + \mathcal{O}\left[\left(\frac{h}{L}\right)^2\right], \qquad \text{[8]}$$

which gives rise to the left-hand side of Eq. 3 with $\Gamma = 12\bar{\eta}/h^2$. Crucially for our subsequent discussion, we note that this averaged, 2D viscous force density is of zeroth order in gradient despite the fact that its 3D counterpart is proportional to $\bar{\nabla}^2$. Indeed, in the process of averaging each vertical gradient $\bar{\partial}_z$ is effectively replaced by a factor proportional to $1/h$, and the horizontal gradients drop out because they are subdominant in the $h \ll L$ limit. Although the prefactor of Eq. 8 assumes a Poiseuille profile for the flow, only the numerical coefficient in its right-hand side and thus the definition of Γ change if other kinds of flows are considered.

In 3D active fluids, this viscous force density is balanced by the divergence of active stresses. This divergence can be expressed in terms of 3D nematic order parameter $\bar{\mathbf{Q}}(\bar{\mathbf{r}}, t)$ as

$$\bar{\nabla} \cdot \bar{\boldsymbol{\sigma}} = \bar{\nabla} \cdot \left(\bar{\zeta}_0 \Delta\mu \bar{\mathbf{I}} - \bar{\zeta}_1 \Delta\mu \bar{\mathbf{Q}} - \bar{\zeta}_2 \Delta\mu \left\{\bar{\nabla}\left[\bar{\mathbf{Q}} \cdot (\bar{\nabla} \cdot \bar{\mathbf{Q}})\right]\right\}^S\right). \qquad \text{[9]}$$

Here the superscript S denotes the symmetric part of a tensor and $\bar{\mathbf{I}}$ denotes the unit tensor. While the two first terms in the right-hand side of Eq. 9 are standard, the last term would be disregarded in a gradient-expansion treatment of an unconfined 3D fluid. Indeed, while the former are of first order in the 3D gradient $\bar{\nabla}$, the latter is of order three. However, similar to the thickness-averaged viscous force density of Eq. 8, its thickness-averaged counterpart gives rise to lower (first)-order terms in horizontal gradient and thus cannot be neglected. This term thus gives rise to the second activity constant ζ_2 discussed in previous sections. To see this more clearly, note that one of the terms arising from the force $\bar{\nabla}_j\left\{\bar{\nabla}_i[\bar{\mathbf{Q}} \cdot (\bar{\nabla} \cdot \bar{\mathbf{Q}})]_j\right\}^S$ is $\bar{\nabla}^2\left[\bar{\mathbf{Q}} \cdot (\bar{\nabla} \cdot \bar{\mathbf{Q}})\right] \approx \bar{\partial}_z^2\left\{\bar{\mathbf{Q}} \cdot (\bar{\nabla} \cdot \bar{\mathbf{Q}})\right\}$. To average this and other terms, we supplement the standard procedure described for the viscous force density with a mean-field treatment whereby the z average of a product of two fields is approximated by the product of their individual z averages (*SI Appendix, II. Derivation of Effective Two-Dimensional Equations of Motion from Three-Dimensional Equations for Active Fluids Confined in One Direction*). Denoting the z-averaged projection of the apolar order parameter onto the xy plane as

$$\mathbf{Q}(\mathbf{x}, t) = \frac{S}{2}\begin{pmatrix} \cos 2\theta & \sin 2\theta \\ \sin 2\theta & -\cos 2\theta \end{pmatrix}, \qquad \text{[10]}$$

the vertical average of the divergence of the third term in the right-hand-side of Eq. 9 contributes a 2D force density of the form $\mathbf{Q} \cdot (\nabla \cdot \mathbf{Q})$ to the thickness-averaged force balance equation. As this contribution is of the same order in 2D gradient as the standard active force density $\nabla \cdot (\bar{\zeta}_1 \Delta\mu \mathbf{Q})$, it must be retained in a 2D description.

Performing this averaging procedure on the evolution equation for the 3D nematic order parameter as well as the force balance equation (*SI Appendix, II. Derivation of Effective Two-Dimensional Equations of Motion from Three-Dimensional Equations for Active Fluids Confined in One Direction*), we obtain the full thickness-averaged 2D dynamical equations

$$\partial_t \mathbf{Q} = -\mathbf{v} \cdot \nabla \mathbf{Q} + \boldsymbol{\omega} \cdot \mathbf{Q} - \mathbf{Q} \cdot \boldsymbol{\omega} - \lambda \mathbf{U} - \Gamma_\theta \mathbf{H}, \qquad \text{[11a]}$$

$$\Gamma \mathbf{v} = -\nabla\Pi - \lambda\nabla \cdot \mathbf{H} - 2\nabla \cdot (\mathbf{Q}\mathbf{H})^A,$$
$$- \zeta_1 \Delta\mu\nabla \cdot \mathbf{Q} - 2\zeta_2 \Delta\mu \mathbf{Q} \cdot (\nabla \cdot \mathbf{Q}), \qquad \text{[11b]}$$

where $\zeta_1 = \bar{\zeta}_1$ and $\zeta_2 = 9\bar{\zeta}_2/h^2$. The thickness-averaged dynamics of the concentration field are described by Eq. 6. These equations reduce to Eqs. 1–5 deep in the ordered phase where S relaxes within a microscopic time to its steady-state value, which we set to 1 without loss of generality. In Eq. 11 $\mathbf{H}$ is the molecular field conjugate to $\mathbf{Q}$, the superscript A denotes the antisymmetric part of a tensor, and $\boldsymbol{\omega}$ and $\mathbf{U}$ are, respectively, the antisymmetric and symmetric parts of the tensor $\nabla \mathbf{v}$. The pressure Π imposes incompressibility as in Eq. 3. Eq. 11 demonstrates that the force $\propto \zeta_2$ previously introduced through general symmetry arguments is a natural emergent feature of confined 3D active dynamics. Note that while we have included only one term of order $\bar{\nabla}^2$ in Eq. 9 for clarity, other $\mathcal{O}(\bar{\nabla}^{n\geq 2})$ terms also contribute both to this extra ζ_2 active force and to the usual ζ_1 one upon thickness averaging and do not introduce any qualitatively new term. Dimensionally, each additional factor of ∇ in the 3D theory must be accompanied by a prefactor of order ℓ, a length scale given by the size of the suspended particles. Meanwhile, similar to Eq. 8 each vertically averaged gradient yields a factor $1/h$. We thus expect $\zeta_2/\zeta_1 \sim (\ell/h)^2$. As a result, in closely confined suspensions with $h \sim \ell$ the coefficients ζ_2 and ζ_1 should be comparable in magnitude.

Dominance and Generality of the Extra Active Force

Beyond these microscopic considerations, we predict that the ζ_2 force will dominate over the old ζ_1 force in a renormalized theory in the presence of noise. Indeed, according to Eqs. 10 and 11b the latter reads $\nabla \cdot \mathbf{Q} = \cos 2\theta(\partial_y \theta \hat{x} + \partial_x \theta \hat{y})$ in the ordered phase, while the former takes the form $2\mathbf{Q} \cdot (\nabla \cdot \mathbf{Q}) = \partial_y \theta \hat{x} - \partial_x \theta \hat{y}$ that does not involve the anisotropic factor $\cos 2\theta$. Since active nematics have only quasi–long-range order, all anisotropic terms average to zero at large scales due to rotation invariance (17), implying that $\langle\cos 2\theta\rangle$ decays as a power of system size with a typically small exponent. Therefore, for large systems, the isotropic ζ_2 active force does not vanish with diverging system size (*SI Appendix, III. Beyond Linear Theory: Scaling of Active Force with Distance*) and thus dominates over the ζ_1 force.

In addition to its role in nematic and polar systems, the active force introduced here is the key to characterizing activity in higher-symmetry active systems, including tetratic (5) and hexatic (26, 27) phases, as expected from the schematic of Fig. 1C. In these systems symmetry imposes that ζ_1, ζ_c, and λ in Eqs. 1–6 all vanish, implying that our ζ_2 term is the only possible source of active instabilities. It arises through an antisymmetric piece of the active stress, proportional in two dimensions to $\theta\boldsymbol{\epsilon}$ in the $\theta \ll 1$ limit, where the pseudoscalar angle field θ is the broken-symmetry mode and $\boldsymbol{\epsilon}$ is the 2D Levi–Civita

tensor. While this does not give rise to a generic instability, these active p-atics on substrates are nevertheless unstable for $\zeta_2 \Delta\mu < -2\Gamma\Gamma_\theta K$ irrespective of the presence of an incompressible solvent. In addition, the aforementioned pure-curl character of the ζ_2 term means that they do not contribute to mass currents. Active tetratics and hexatics thus have normal (nongiant) number fluctuations.

Dynamics of Defects

Beyond linear stability analysis, activity in orientable fluids also modifies the dynamics of defects. In nematics, the most abundant defects have charges $+1/2$ and $-1/2$. It is well known that $+1/2$ defects are motile in active nematics (5, 28–30). The ζ_2 active force does not lead to any additional propulsion of these defects. Indeed, the force density generated by this term is isotropic, $(\zeta_2 \Delta\mu/2r)\hat{r}$, and thus cannot lead to defect propulsion. Similarly, in systems with higher symmetry where only the ζ_2 term is allowed, defects parameterized as $\theta = \pm n\psi$ in polar coordinates (r, ψ) (with $n = 1/4$ for tetratics and $n = 1/6$ for hexatics) lead only to an isotropic active force density. Therefore, ballistic motion of defects is impossible in such higher symmetry systems.

Experimental Consequences and Discussion

The presence of the ζ_2 active term has measurable implications for current experiments on biological active matter. First and foremost, we predict the existence of stable states for arbitrarily high values of the activity parameter $\Delta\mu$. This helps rationalize the recent observation of highly ordered apolar nematic phases in confined suspensions of *Escherichia coli* bacteria (19). The absence of bacterial turbulence in these systems would have been a puzzle in a treatment with a single activity parameter ζ_1. Indeed, the experiments use a nontumbling mutant, i.e., a system with a highly reduced Γ_θ in Eq. 7, which should favor instability. The resolution could well lie in our mechanism involving a second activity parameter with a possibly stabilizing effect.

While this qualitative prediction helps explain the persistence of stable states in situations with high activity or low dissipation, it is not sufficient to determine whether the aligned state in a given experiment is stable due to our mechanism or because the largest experimentally accessible $\Delta\mu$ is simply too small. To discriminate between these two possibilities, we note that in a noisy environment the stabilizing influence of the ζ_2 active term on the diffusivity $D(\phi)$ given in Eq. 7 is directly reflected in the magnitude of the angular fluctuations even within a stable aligned state. Considering an angular noise strength $2T\Gamma_\theta$, our theory thus predicts that the equal-time correlator for angular fluctuations reads

$$\langle \theta_q(t)\theta_{-q}(t)\rangle = \frac{T\Gamma_\theta}{D(\phi)q^2}. \qquad [12]$$

In a theory including only the old ζ_1 active term, an increase of the ratio $\Delta\mu/\Gamma$ (e.g., through an increase of the amount of ATP available in a cytoskeletal assay) should lead to a decrease of this correlator along certain directions ϕ and an increase along others. By contrast, in the presence of the stabilization mechanism discussed here (i.e., for $\zeta_2 > |\zeta_1|$), this correlator will decrease along all directions ϕ, providing a quantitative test for the existence of the ζ_2 stabilization.

Our linear stability analysis also helps to heuristically understand pattern formation in bacterial and cytoskeletal active fluids (10, 11, 31, 32). The anisotropy of $D(\phi)$ in Eq. 7 implies that the ordered phase is destabilized when it first becomes negative for any angle ϕ_u. In this case, bands with the normal vector oriented along ϕ_u are likely to form whose length scale can be obtained simply by extending, to fourth order in

the wavenumber q, the 2D mode analysis that led to Eq. 7. The resulting dynamics read $\partial_t \delta\theta_{\mathbf{q}} = -[D(\phi)q^2 + K_r(\phi)q^4]\delta\theta_{\mathbf{q}}$, where the stabilizing coefficient $K_r(\phi) = (K/4\Gamma)(1 - \lambda\cos 2\phi)^2$ arises simply from Frank elasticity and thus accounts for patterns with size $\approx \sqrt{K_r(\phi_u)/|D(\phi_u)|}$ without resorting to previously invoked ad hoc high-order gradient expansions (11, 32, 33). Moreover, when the effective 2D dynamics are those of a confined 3D fluid as discussed above, $\Gamma \propto 1/h^2$ so that K_r dominates over such ad hoc terms by a factor $\mathcal{O}(h/\ell)^2$, which can be large depending on the scale of the confinement.

Beyond these applications, this order-q^4 theory can be extended to explain ordering and pattern formation in novel "living liquid crystals," namely passive nematic liquid crystals with well-characterized physical properties perfused with small quantities of bacteria. Because of the small amount of active bacteria in them, these systems share most of their passive properties with the embedding, often well-characterized liquid crystal. This offers unprecedented opportunities to quantitatively test our and other theoretical predictions. The detailed connection between these systems and the current study is discussed in *SI Appendix, IV. Living Liquid Crystals*, where we introduce two coupled angle fields for the local alignment of the passive liquid crystalline particles and active bacterial ones. Our approach accounts for activity without the need for previously introduced ad hoc Onsager symmetry-breaking orientational couplings between these two angular fields (20) and leads to a stability criterion identical to that of Eq. 7. As a quantity analogous to λ can be quantitatively tuned by modifying the passive properties of the liquid crystal, our stability prediction is directly testable, and we predict the appearance of patterns with a similarly tunable length scale. Changing the embedding liquid crystal, the viscosity of the solvent, or the scale of the confinement should also enable modifications of the parameters analogous to K, Γ, and Γ_θ in Eq. 7 and allow direct tests of whether a flow-tumbling system with a large and positive ζ_2 remains stable when $\Delta\mu/(K\Gamma\Gamma_\theta) > 2$, as we predict.

Finally, our approach suggests an explanation for the recent observation (34) that the transition to activity-driven turbulence in extensile microtubule–kinesin systems confined in a channel is controlled by the aspect ratio of the transverse cross-section of this channel. Averaging the dynamics over the z direction in a channel with a rectangular $L_y \times h$ cross-section, we look at the longest wavelength splay fluctuations in the y direction, while noting that extensile particles imply $\bar{\zeta}_1 > 0$, which stabilizes splay fluctuations. Assuming a destabilizing $\bar{\zeta}_2 < 0$, we predict that the system should become unstable as h is decreased and the ratio $\zeta_2/\zeta_1 \propto 1/h^2$ subsequently increases. We therefore predict that ζ_2 active force plays a destabilizing role in microtubule–kinesin systems.

1. Kruse K, Joanny JF, Jülicher F, Prost J (2006) Contractility and retrograde flow in lamellipodium motion. *Phys Biol* 3:130–137.
2. Hakim V, Silberzan P (2017) Collective cell migration: A physical perspective. *Rep Prog Phys* 80:076601.
3. Ballerini M, et al. (2008) Interaction ruling animal collective behavior depends on topological rather than metric distance: Evidence from a field study. *Proc Natl Acad Sci USA* 105:1232–1237.
4. Saha S, Golestanian R, Ramaswamy S (2014) Clusters, asters, and collective oscillations in chemotactic colloids. *Phys Rev E* 89:062316.
5. Narayan V, Menon N, Ramamswamy S (2007) Long-lived giant number fluctuations in a swarming granular nematic. *Science* 317:105–108.
6. Ramaswamy S (2017) Active matter. *J Stat Mech* 2017:054002.
7. Marchetti MC, et al. (2013) Hydrodynamics of soft and active matter. *Rev Mod Phys* 85:1143–1189.
8. Toner J, Tu Y, Ramaswamy S (2005) Hydrodynamics and phases of flocks. *Ann Phys* 318:170–244.
9. Schaller V, Weber C, Semmrich C, Frey E, Bausch AR (2010) Polar patterns of driven filaments. *Nature* 467:73–77.
10. Sanchez T, Chen D, DeCamp SJ, Heymann M, Dogic Z (2012) Spontaneous motion in hierarchically assembled active matter. *Nature* 491:431–434.
11. Dunkel J, Heidenreich S, Bär M, Goldstein RE (2013) Minimal continuum theories of structure formation in dense active fluids. *New J Phys* 15: 045016.
12. Simha RA, Ramaswamy S (2002) Hydrodynamic fluctuations and instabilities in ordered suspensions of self-propelled particles. *Phys Rev Lett* 89:058101.
13. Voituriez R, Joanny JF, Prost J (2005) Spontaneous flow transition in active polar gels. *Europhys Lett* 70:404–410.
14. Marenduzzo D, Orlandini E, Cates ME, Yeomans JM (2007) Steady-state hydrodynamic instabilities of active liquid crystals: Hybrid lattice Boltzmann simulations. *Phys Rev E* 76:031921.
15. Kumar A, Maitra A, Sumit M, Ramaswamy S, Shivashankar GV (2014) Actomyosin contractility rotates the cell nucleus. *Sci Rep* 4:3781.
16. Ramaswamy S, Simha RA, Toner J (2003) Active nematics on a substrate: Giant number fluctuations and long-time tails. *Europhys Lett* 62:196–202.
17. Shankar S, Ramaswamy S, Marchetti MC (2018) Low-noise phase of a two-dimensional active nematic system. *Phys Rev E* 97:012707.
18. Mishra, S (2008) *Dynamics, order and fluctuations in active nematics: Numerical and theoretical studies*. Available at www.openthesis.org/documents/Dynamics-order-fluctuations-in-active-601122.html. Accessed August 20, 2017.
19. Nishiguchi D, Nagai KH, Chaté H, Sano M (2017) Long-range nematic order and anomalous fluctuations in suspensions of swimming filamentous bacteria. *Phys Rev E* 95:020601.
20. Zhou S, Sokolov A, Lavrentovich OD, Aranson IS (2014) Living liquid crystals. *Proc Natl Acad Sci USA* 111:1265–1270.
21. Prost J, Marcerou (1977) On the microscopic interpretation of flexoelectricity. *J Phys France* 38:315–324.
22. Meyer RB (1969) Piezoelectric effects in liquid crystals. *Phys Rev Lett* 22:918–921.
23. Bricard A, Caussin JB, Desreumaux N, Dauchot O, Bartolo D (2013) Emergence of macroscopic directed motion in populations of motile colloids. *Nature* 503:95–98.
24. Stone HA (2002) *Nonlinear PDEs in Condensed Matter and Reactive Flows*, NATO Science Series C: Mathematical and Physical Sciences, eds Berestycki H, Pomeau Y (Kluwer Academic, Dordrecht, The Netherlands), Vol 569.
25. Oron A, Davis SH, Bankoff SG (1997) Long-scale evolution of thin liquid films. *Rev Mod Phys* 69:931–980.
26. Redner GS, Hagan MF, Baskaran A (2013) Structure and dynamics of a phase-separating active colloidal fluid. *Phys Rev Lett* 110:055701.
27. Palacci J, Sacanna S, Steinberg AP, Pine DJ, Chaikin PM (2013) Living crystals of light-activated colloidal surfers. *Science* 339:936–946.
28. Giomi L, Bowick MJ, Ma X, Marchetti MC (2013), Defect annihilation and proliferation in active nematics. *Phys Rev Lett* 110:228101.
29. Pismen L (2013) Dynamics of defects in an active nematic layer. *Phys Rev E* 88: 050502.
30. Giomi L, Bowick MJ, Mishra P, Sknepnek R, Marchetti MC (2014) Defect dynamics in active nematics. *Philos Trans R Soc A* 372:20130365.
31. Giomi L (2015) Geometry and topology of turbulence in active nematics. *Phys Rev X* 5:031003.
32. Oza AU, Dunkel J (2016) Antipolar ordering of topological defects in active liquid crystals. *New J Phys* 18:093006.
33. Srivastava P, Mishra P, Marchetti MC (2016) Negative stiffness and modulated states in active nematics. *Soft Matter* 12:8214–8225.
34. Wu K-T, et al. (2017) Transition from turbulent to coherent flows in confined three-dimensional active fluids. *Science* 355:eaal1979.